Homogeneous succinylation of cellulose acetate: Design, characterization and adsorption study of Pb(II), Cu(II), Cd(II) and Zn(II) IONS

Chahid Zannagui [1*], *Hassan* Amhamdi[1], *Soufian* El Barkany[2], *Issam* Jilal[2], *Ola* Sundman[3], *Amin* Salhi[4], *Mohamed* Abou-Salama[2], *Abderahmane* El Idrissi[4]

[1]Laboratory of Research and Development in Engineering Sciences, Unit of Applied Chemistry, Faculty of Sciences and Techniques, Abdelmalek Essaadi University, 32 003 Al Hoceima, Morocco
[2]Multidisciplinary Faculty of Nador, Department of Chemistry, Mohamed first University, 60700 Nador, Morocco
[3]Department of Chemistry, Umeå University, Sweden
[4]Laboratory of Applied Chemistry and Environmental (LCAE-URAC18), Faculty of Sciences of Oujda, Mohamed 1st University, 60000 Oujda-Morocco

Abstract. In this study, the removal of Pb(II), Cu(II), Cd(II), and Zn(II) ions from aqueous solutions was investigated using succinic anhydride modified cellulose monoacetate. In the first part, the cellulose acetate was successfully succinylated in a homogenous medium of DMF using 4-dimethylaminopyridine (DMAP) as a catalyst. The obtained material (AcS) was analyzed by FTIR and CP/MAS ^{13}C NMR Spectroscopy, thermogravimetry analysis and DRX patterns. The titration method was used to determinate the degree of hydroxyl group substituted by carboxyl group (DS) and was found to be 1.36. In the second part, the Bach technique was used to study the effects of pH, contact time, concentration of metals, ionic selectivity and regeneration. Maximum sorption capacities of AcS for Pb(II), Cu(II), Cd(II), and Zn(II) were 241.81, 133.76, 156.61 and 73,58 $mg.g^{-1}$, respectively. The Langmuir isotherm and the pseudo second order kinetic models provided best fit to the experimental data of metal ion sorption. The nature of the adsorption process was exothermic and spontaneous in nature with negative values of $\Delta G°$ and $\Delta H°$. Regeneration of the modified cellulose acetate was accomplished using nitric solution and showed high stability and good recyclability.

1 Introduction

Water pollution remains a noteworthy worry of society, and that is due to the presence of high concentrations of wide assortments of contaminants and pollutants, for example, toxic heavy metal ions, micropollutants, inorganic anions, and organic compounds (humic substances, phenols, detergents, dyes, pesticides, etc.). The heavy metals are very dangerous and they are among the most hazardous particles since they are not biodegradable and very toxic [1-3], even though to a very small range of concentration, they are known for their tendency to bioaccumulation [4], causing different clutters and diseases [5-7]. The heavy metals are discharged into the environment by anthropic activities, in any case, these substances can enter a water supply by industrial and consumer waste, or from acidic rain cracking soils caused the clearance of heavy metals into streams, rivers, lakes, and groundwater [1, 8, 9]. A few depollution processes, such as physical and chemical processes, have been developed keeping in mind the end goal to limit or minimize the elimination of these hazardous compounds, such as chemical precipitation [10], electrochemical method [11], ion exchange[12], reverse osmosis [13, 14] and membrane separation [15]. So far, most of these techniques remain costly and less adapted, and the adsorption is the most extensively used technique for its high efficiency and easy processing. Moreover, using the materials of biological origin is viewed as the best technique for eliminating heavy metal ions because they have several advantages such as a low cost, biodegradable, high availability, and numerous functional groups that can easily be modified by simple chemical reactions [16-18]. In this area, cellulose-based adsorbents brought more attention [19].

Certainly, cellulose is the most abundant linear natural polymer, renewable, biodegradable, biocompatible, and modified chemically to yield various useful products. Yet, little research uses cellulose as a chemical raw material because of its insolubility resulting principally from strongly lengthy intermolecular hydrogen bonds of cellulose repeat units [16, 20-23].

In recent years, several materials based on the cellulose surface modification were currently used to remove heavy metal ions from aqueous solutions, for exemple, thio- and/or amine-modified cellulose has shown an adsorption capacity of 104.2, 69.3 and 30.8 for Cu(II), Zn(II) and Ni(II), respectively [21, 24]. Furthermore, the acrylonitrile grafted cellulose was widely used as an adsorbent for heavy metal removal [25, 26]. However, modified cellulose by succinic anhydride and by maleic anhydride showed encouraging results, which the maximum metal uptake was found to be 294.1, 164.0 and 123.5 mg/g for Pb(II), Cd(II) and Cu(II), respectively.

*Corresponding author: chahidzannagui@gmail.com

This study describes the preparation and evaluation of succinic anhydride modified cellulose monoacetate for the adsorption of Pb(II), Cu(II), Cd(II) and Zn(II) ions from aqueous solutions. The new modified cellulose materials were analyzed and characterized by the back titration and the structural spectroscopic techniques (FTIR, ^{13}C and ^{1}H NMR, TGA/DTA, XRD and SEM). The surface morphology was analyzed using the thermal stability, SEM, and crystallinity changes were discussed based on in TGA thermograms and X-ray diffraction XRD patterns, respectively. The adsorption capacity of AcS material to remove Pb(II), Cu(II), Cd(II) and Zn(II) ions from aqueous solutions was evaluated using the Batch technique. The experimental data were fitted to kinetic pseudo-first and pseudo-second order models. The adsorption isotherms were studied using Langmuir and Freundlich models. The thermodynamic parameters of adsorption processes (ΔG°, ΔH° and ΔS°), selectivity and regeneration studies were also examined.

2 Materials and methods

2.1 Materials

Cellulose powder was purchased from HIMEDIA Company. The succinic anhydride, pyridine and acetic anhydride were obtained from Sigma Aldrich. 4-diméthylaminopyridine (DMAP) and N,N-Dimethylacetamide (DMAc) were purchased from Sigma-Aldrich Company, ethanol and KOH were obtained from Merck. All other chemicals indicated in these experiments were analytical grade reagents and were used without any purification. The stock solution of metals was prepared with deionized water. The prepared solution of HCl (0.1N) and NaOH (0.1N) was used for pH adjustment.

2.2 Methods

The chemical structure was evaluated using the Fourier Transform Infrared (FTIR) technique. The spectra were performed on *Shimadzu FTIR-8400S FTIR* spectrometer using the KBr pellets of finely ground with 2% of the sample at a resolution of 2 cm^{-1}. An average of 40 scans was taken for each sample and recorded from 4000 to 400 cm^{-1}. ^{1}H and ^{13}C NMR measurements were performed on a Bruker spectrometer at 360 °K, using TMS as internal standard and DMSO-d_6 as Solvent. ^{13}C MAS NMR spectra were obtained with cross polarization (CP) using a 3 μs^{1}H excitation pulse, followed by 1.5 ms cross polarization with a 62.5 kHz spin lock on ^{13}C and a ramped ^{1}H spin lock (41-82 kHz) and subsequently high power ^{1}H decoupling at 83 kHz using the *SPINAL-64* sequence during acquisition. The acquisition time was 6.8ms and was followed by a relaxation delay of 2 s. The number of scans was typically 1800. The crystallinity of each sample was studied by X-ray diffraction technique and the analysis was recorded on an X-ray Diffractometer *EQUINOX 2000* using copper radiation CuK_α (λ= 1.5418 A°), at an accelerating voltage of 40 kV and an operating current of 30 mA. All patterns were recorded in the range of 2θ (10°-40°). 0.25 g of each sample was pressed under 50 MPa to form the pellets of an average of 25 mm in diameter. The SEM images were obtained on a FEI-Quanta 200. The thermal stability and the mass loss determinations were performed under air in a platinum crucible on a *PerkinElmer Diamond* TG/DTA at a heating rate of 10 °C min^{-1}.

2.3 Synthesis of succinic anhydride modified cellulose monoacetate

Cellulose monoacetate (Ac1) with a DS~1 was prepared and characterized using the methodology described by to Elidrissi et al. [27]. To an optically clear solution of Ac1 (5 g, 18 mmol) dissolved in DMAc (50 mL) at 80 °C for 2 h with continuous stirring, succinic anhydride (10.82 g, 108 mmol) was added. Then the DMAP (250 mg, 2.05 mmol) was added as a catalyst. The reaction was kept under stirring at 80 ° C for 24 h. The reaction mixture was precipitated in diethyl ether to obtain AcS. The product was filtered, washed with acetone and treated with a saturated solution of $NaHCO_3$ and stirred at room temperature for 2h to liberate carboxylate functions for a better chelating function. After filtration, the AcS was washed with distilled water several times until the filtrate became neutral, then washed with ethanol 95%, acetone and dried in an oven for 6 hours at 70 °C.

2.4 Determination of carboxyl content and Degree of succinylation

The percentage of succinic acid introduced was determined by the back titration by measuring the concentration of introduced carboxylic functions per gram of modified cellulose. For this, an amount of 0.1g of AcS was dispersed in 100 mL of $NaHCO_3$ solution (0.01 N) and kept at room temperature under stirring for 7 h. After the saponification of carboxyl groups, the materials were separated by single filtration and three aliquots (25 mL) of each obtained solution was titrated with HCl solution (0.01N). The amount of introduced carboxylic groups per AGU of AcS (C−COOH (mol.g^{-1})) was obtained using the following equation (eq.1):

$$C_{COOH}(mol.g^{-1}) = \frac{4\left(N_{NaHCO3}V_{NaHCO3} - N_{HCl}V_{eq}\right)}{W_{AcS}} \quad (1)$$

where, N_{NaHCO3} is the Normality of $NaHCO_3$ solution (0.01N), V_{NaHCO3} is the volume of $NaHCO_3$ solution. N_{HCl} is the Normality of HCl solution used to titrate the excess of unreacted $NaHCO_3$ and W_{AcS} is the weight of AcS.

eq. 1 was developed to insert the DS parameter which is expressed by the eq. 2:

$$DS = \frac{C_{COOH}.209}{3-[C_{COOH}.82]} = 1{,}36 \quad (2)$$

2.5 Batch experiments

The adsorption capacity of AcS to remove Pb(II), Cu(II), Cd(II) and Zn(II) from aqueous solutions, was studied using 10 mg of the adsorbent (AcS) and 10 mL of the metal aqueous solution. The metal ion concentrations were varied from 10 to 500 mg. L^{-1} and the effect of pH was studied in the range of 1 to 7. The kinetic study was carried out by varying contact time from 5 to 60 min and the agitation was conducted under magnetic stirring at room temperature (25 °C). At the equilibrium, the solid phase was separated by centrifugation and the supernatant was recovered. The residual metal concentration was measured by flame atomic absorption (*ThermoScienific iCE3000, Type iCE3500AA System*). The adsorption capacity was expressed by the amount of metal ions adsorbed per unit mass of modified cellulose ($mg.g^{-1}$) using the following equation (eq. 3):

$$q_M = (C_0 - C_e) \times \frac{V}{M} \quad (3)$$

where q_M is the amount of the metal ion adsorbed ($mg.g^{-1}$), C_0 and C_e are the initial and the equilibrium concentrations (mg. L^{-1}), respectively. M and V are the weight of the adsorbent (mg) and the volume of the solution (L), respectively.

3 Results and discussion

The synthesis path used to prepare the new AcS materials was exemplified in Figure 1. The synthesis strategy of the AcS adsorbents was divided into two parts; the first part consisted of solving the problem of the solubility of cellulose polymer by the fractionated acetylation of the hydroxyl groups according to the method described by *El Idrissi et al. 2012* [27], in which the deacetylation allowed for the liberation of 50% of C_6-OH, whereas, the succinylation occurred in homogeneous medium and allowed us to obtain a high carboxyl content.

This strategy allowed the introduction of carboxylic functional groups capable to adsorbing metal ions through ion exchange and complexation.

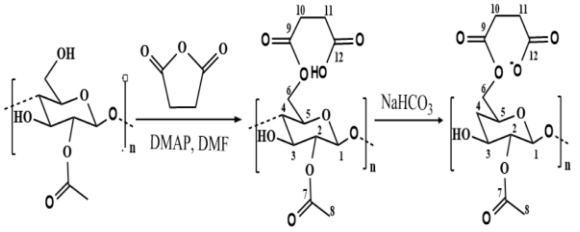

Fig. 1. Synthesis route used to obtain AcS.

3.1 FTIR characterization

The FTIR spectra of Ac1 and AcS are shown in Figure 2. The spectrum of Ac1 showed that the cellulose acetate presents two important peaks, the first one appeared at 1749 cm^{-1} which is attributed to the axial deformation of carbonyl ester $(C=O)_{ester}$ [28, 29], while the second was located at 1232 cm^{-1} which can be related to the absorption stretching of the $(C\text{-}O)_{ester}$ group [30, 31]. The broad absorption peaks at 3420 and 3450 cm^{-1} were due to the hydroxyl group (–OH) stretch while the peak at 2,890 cm^{-1} was related to the C–H vibration of–CH_2 groups. The comparison between the spectra of Ac1 and AcS revealed the appearance of a new band at 1594 cm^{-1}, which attributed to carbonyl stretching of carboxylate (COO^-Na^+) ions coming from introduced succinic acid. The presence of the carboxylate carbonyl in the products was also confirmed by the typical absorption at 1409 cm^{-1}, arising from the carbonyl symmetric stretching vibration [32]. The band at 1,724 cm^{-1} was due to the stretching of carboxyl group (C=O). The bands at 1,158, 1112 and 1,060 cm^{-1} are attributed to the ether bond increase. The appearance of these new bands related to the introduction of new carbonyl groups in Ac1 indicated that the succinylation reaction successfully occurred.

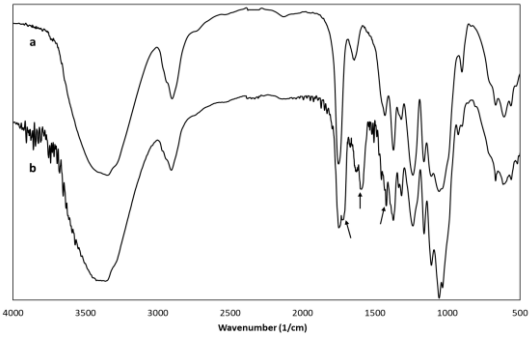

Fig. 2. FITR spectra of Ac1 (a) and AcS (b).

3.2 ^1H and ^{13}C NMR and ^{13}C CP/MAS NMR

The ^1H-NMR spectrum of Ac1 (Figure 3a) first showed, the multiple bands in the region of 3.25–5.3 ppm which were attributed to the AGU protons [33, 34], strong signals within the chemical shift range from 1.8 to 2.2 ppm attributed to the methyl protons of acetyl groups (C_2, C_3 and C_6) [3, 4, 33, 34].

The distribution of the acetyl moiety among the three OH groups in AGU can be calculated from the quantitative integration of acetyl methyl protons areas of the ^1H NMR spectrum roughly [30].

The spectrum of Ac1 showed three signal types (Figure 3b), the signals located in the range from 60 to 104 ppm belong to the AGU and the solvent DMSO-d_6.

The methyl carbons exhibited three signals at around 20 ppm, and the carbonyl carbons showed signals around 169 ppm. The carbon signals at 169.8, 168.9 and 168.6 are attributed to C=O of C6, C3 and C2, respectively. The picks at 103.2, 99.4, 80.3, 75.8, 70.3−73.4, 62 ppm and 60.2 ppm are attributed to C1, C1', C4, C4', the combined C2, C3, and C5, and finally, C6' and C6 of AGU, respectively. The strong peaks at 20 ppm are allocated to the carbons of methyl (CH_3).

In the CP/MAS (solid-state) ^{13}C NMR spectrum of AcS (Figure 3c), the most relevant change observed comparing to Ac1 was the appearance of two signals at 173.78 and 30.52 ppm. The first signal at 173.78 was due to the carbon of carboxylic groups (C12) and the second at 30.52 ppm corresponded to methylene carbons (C10 and C11).

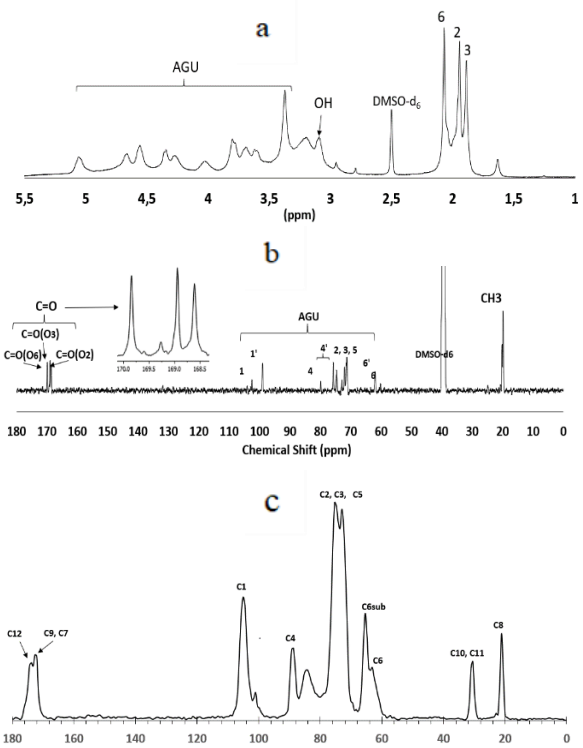

Fig. 3. ^{1}H NMR spectra of Ac1 (a); ^{13}C NMR of Ac1 (b) and Solid-state ^{13}C CP/MAS NMR spectra of AcS (c).

3.3 TGA analysis and thermal stability

TGA and DTA curves of Ac1 and AcS are presented in Figure 4. However, cellulose monoacetate was degraded in three steps; the first step was noted from the room temperature (25 °C) to 130 °C in which was displayed a minor weight loss owing to water desorption, which corresponded to an endothermic peak, in the DTA curves around 62 °C. The second step represented the most important degradation, it was attributed to the main thermal degradation of the cellulose monoacetate chains and was considered starting at 277 °C. The highest rate of weight loss of Ac1 happened at 358 °C [27].

Besides, the carbonization of Ac1 to ash, which consisted of the last step starts at 390 °C. The thermograms of AcS showed that the introduction of succinic acid moieties onto the cellulosic fibers decreased their thermal stability. Indeed, the degradation temperature (Td) decreased from 358 °C to 340 °C for Ac1 and AcS samples, respectively. As shown in Figure 4, at 370 °C, the weight loss of Ac1 was about 80 %, while that of AcS was about 65 %. Cellulose acetate has a linear chains, which gave a large part of the formation of hydrogen bonds imparting thermal stability to the polymer, since, the substitution of hydroxyl groups by succinic acid generated the physical separation of cellulose monoacetate chains and resulted in the decrease in the intermolecular interactions which translated by a significant decrease in the thermal stability of AcS [35].

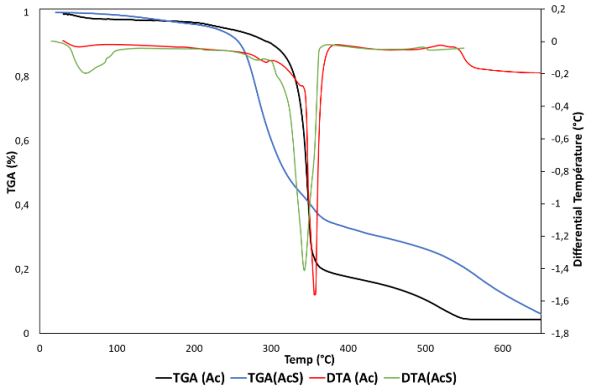

Fig. 4. TGA and DTA spectra of Ac1 and AcS.

3.4 Scanning electron microscopy (SEM)

The surface morphologies of Ac1 and AcS materials are shown in Figure 5 using the SEM analysis. Compared to Ac1, the morphologies of modified cellulose monoacetate showed a remarkable difference in texture and morphology, the surface of AcS was rougher and more irregular than that of the Ac1, which was due to the destruction of hydrogen bonds between macromolecular chains. The specific surface area of AcS became larger because of the heterogeneous surface. Evidently, this situation will be helpful to metal ion absorbed.

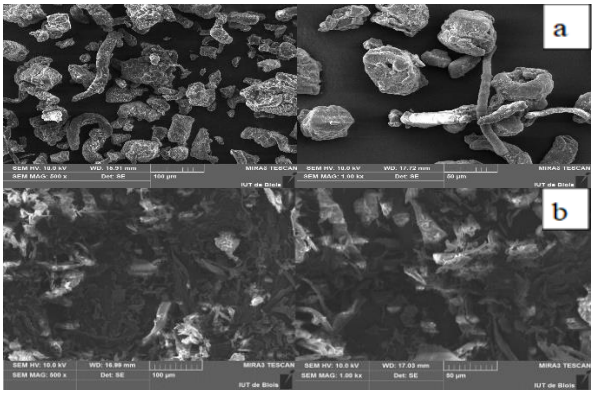

Fig. 5. SEM images of Ac1 (a,) and AcS (b)

3.5 X-ray diffraction

The X-ray diffraction patterns of Ac1 and AcS are shown in Figure 6. The Ac1 showed the Bragg angle diffractions (2-theta) located at around 14.4°, 16.85°, 22.34° and 34.6°, which are attributed to the reticular plans (101) (101) (002) and (040).

Compared to the Ac1 spectrum, the X-ray diffraction spectrum of AcS showed a decrease in the degree of crystallinity after the modification, indicating that the

crystal structure of cellulose acetate was destroyed after modification with succinic acid and this indicated that the density of the hydrogen bond has been successfully decreased and the amorphous character was clearly increased.

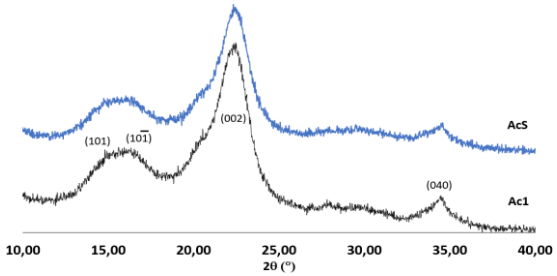

Fig. 6. X-ray diffraction patterns of Ac1 and AcS

3.6 Adsorption capacity of AcS for metal ions

3.6.1 Effect of pH

The removal of metal ions from aqueous solutions using carboxylate functions depends strongly on the pH and the desired pH was determined according to the total saponification of the carboxylic form to the carboxylate one [36].

To study the pH effect on metal removal, the solution pH was varied from 2-7 at T = 25°C, with the contact time of 30 min and optimum concentration of each metal ions. The effect of pH on the adsorption of Pb (II), Cu (II), Cd (II) and Zn (II) onto AcS is shown in Figure 7. Since an increase in the pH value allowed a remarkable augmentation of the adsorption capacities of metal ions on AcS, whereas, at lower pH values, there was a competition on adsorption sites between the metal ions and H^+ ions. As well, the carboxylate functions of material (COO-) must be almost entirely in its protonated form (COOH), in which the predominance of carboxylic form, that caused a decrease in the number of negatively charged sites [37].

Thus, adsorption capacities were found to be lower at lower pH values. At pH>7, the metal ions hydrolysed in the form of hydroxides of $M(OH)^+$ and $M(OH)_2$. Then the maximum adsorption for each metal took place at the pH range of 6 to 7. To avoid any precipitation of metals, the pH 6 value was selected for the other adsorption experiments.

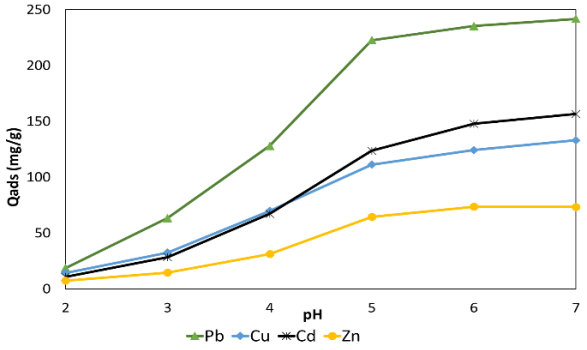

Fig. 7. Effect of pH on adsorption of metal ions by AcS

3.6.2 Effect of contact time and kinetic modeling

The effect of contact time on the adsorption of metal ions by AcS is shown in Fig. 7a. Experiments were performed at the room temperature, at a ~~co~~ntact time ranging from 5 to 60 min and at a pH of 6.0. Yet, during short contact times, the adsorption rate was very fast for all metal ions and the plateau was reached after about 30 min, where the fast extraction rate indicated that the adsorbent was highly suitable for the removal metal ions Pb (II), Cu (II), Cd (II) and Zn (II) from aqueous solutions. This may be due to the presence of numerous active sites on the adsorbent surface. The observed variation in adsorption capacity was probably due to the size of the metals, degree of hydration, forms of the hydroxides formed and the constant of their complexes band with the material.

The kinetics and equilibrium of adsorption, which consists of the important physical-chemical aspects of the process, were used to study the process of adsorption. The pseudo-first-order and the pseudo-second-order kinetic adsorption models were used to analyze the adsorption kinetics (eq.4 and eq.5):

$$ln\ ln\left(q_e - q_t\right) = lnq_e - k_1 t \quad (4): \text{ Pseudo-first order}$$

$$= \frac{1}{k_2 q_e^2} - \frac{k_1 t}{q_e} \quad (5): \text{ Pseudo-second-order}$$

where q_e and q_t are the amounts of metal ions adsorbed ($mg.g^{-1}$) at equilibrium and at time t, respectively, k_1 is the rate constant of the first-order adsorption in min^{-1} and k_2 ($g.\ mg^{-1}\ min^{-1}$) is the pseudo-second-order adsorption rate constant.
The result of kinetic modeling of linear pseudo-second order model is shown in Figure 7b and the values of kinetic parameters are presented in Table 2.

The adsorption kinetic was fitted with the pseudo-second-order kinetic for all metal ions with the values of the correlation coefficient (R^2) close to unity. Besides, the comparison made between the experimental adsorption capacity (q_{exp}) values and the calculated adsorption capacity (qe) values have shown that the calculated qe values were comparable to the experimental q_{exp} values for the pseudo-second order kinetics.

Table 1. Kinetic parameters of the two models applied in metal ion adsorption

Model	Parameters	Pb(II)	Cu(II)	Cd(II)	Zn(II)
Experimental	$q_{e(exp)}$ ($mg.g^{-1}$)	241,64	133,75	156,23	73,91
Pseudo-1er Ordre	q_e ($mg.g^{-1}$)	314,53	225,36	126,94	44,13
	K_1 (min^{-1})	0,249	0,324	0,235	0,134
	R^2	0,816	0,930	0,925	0,921
Pseudo-2eme Ordre	q_e (mg/g)	250,89	143,06	165,29	77,52
	K_2 ($g.\ mg^{-1}\ min^{-1}$)	0,0019	0,0034	0,0031	0,0059
	R^2	0,998	0,997	0,997	0,995

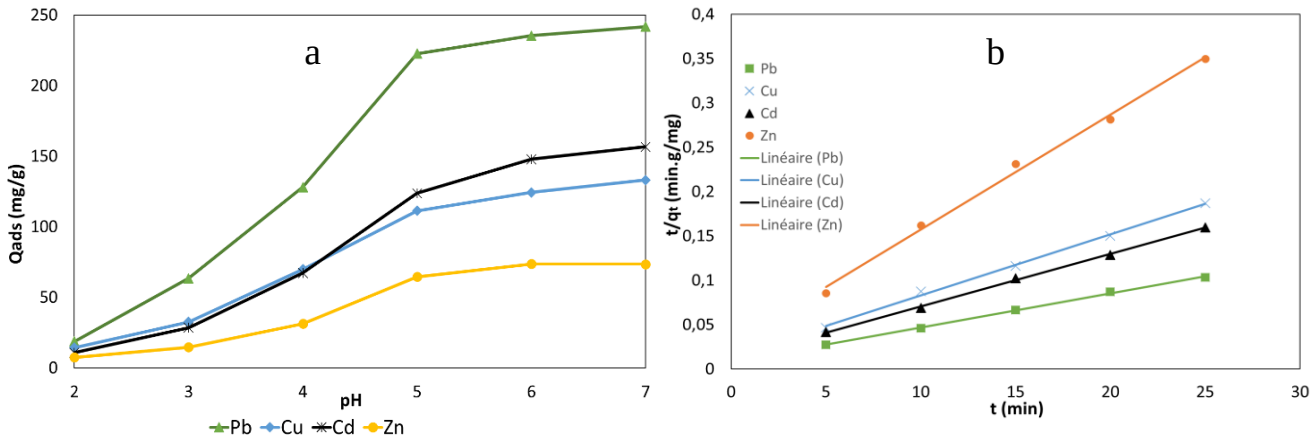

Fig. 8. Effect of contact time of the adsorption of metal ions by AcS (a); Graph of the pseudo-second order kinetic model (b).

3.6.3 Adsorption isotherm modeling and Thermodynamic studies

The effect of the initial Pb (II), Cu (II), Cd (II) and Zn (II) concentration on the adsorption capacity was studied by varying the initial metal ion concentration between 10 and 500 mg. L^{-1} (Figure 9). The adsorption studies were done at room temperature (25°C), pH of 6.0 and at a contact time of 30 min. All the results showed that the lowest metal initial ion concentration solutions were faster and had the highest rate of removal. Increasing the initial metal ion concentrations from 150 to 500 mg.L^{-1}, decreased the rate of adsorption until the adsorption capacity obtained reached the equilibrium state with maximum metal ion uptake, indicating the saturation of the active chelates sites.

The maximum adsorption capacities of metal ions by AcS, were found to be 241.26, 133,49,155,87 and 74,65 mg/g for Pb(II), Cu(II), Cd(II) and Zn(II), respectively.

Two isotherm models were applied namely Langmuir and Freundlich. The Langmuir model that assumes monolayer adsorption of solutes onto a surface comprised of a finite number of identical sites with homogeneous adsorption energy [38].

The Freundlich model proposes a monolayer sorption with heterogeneous energetic distribution of active sites, and/or interactions between adsorbed species [39]. The linear form of Langmuir and Freundlich models are given as follows, respectively:

$$q_e = \frac{qbC_e}{1+bC_e} \quad (6)$$

$$q_e = K_e C_e \quad (7)$$

Equations 6 and 7 can be linearized as follows, respectively:

$$\frac{C_e}{q_e} = \frac{C_e}{q} + \frac{1}{qK_L} \quad (8)$$

$$ln\ ln\ q_e = ln\ ln\ K_e + \frac{1}{n} ln\ ln\ C_e \quad (9)$$

where q_e is the quantity of solute adsorbed (mg.g^{-1}), C_e is the equilibrium concentration ion in the solution (mg.L^{-1}), q (mg.g^{-1}) is the maximum adsorption capacity. K_L (L.mg^{-1}) is the Langmuir constant associated to the free adsorption energy, K_F (mg.g^{-1}) is Freundlich constant associated with the adsorption capacity and n is the Freundlich constant attaches to the adsorption intensity.

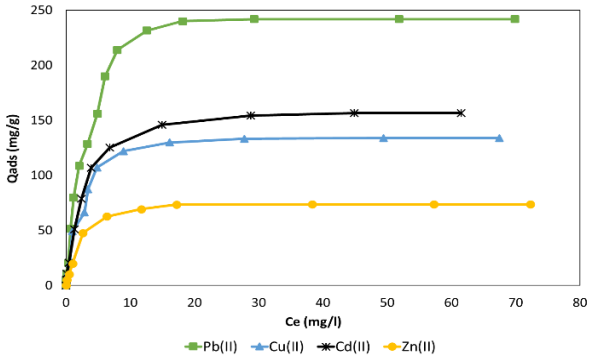

Fig. 9. Effect of the initial concentration of metal ions on the adsorption capacity of AcS.

The isotherm model parameters were calculated from the slopes and intercepts of different straight lines representing the interaction of AcS with different metal ions (Figure 10).

These calculated values are given in Table 3, and show that the equilibrium data fitted as well with Langmuir isotherm.

From these results, the correlation coefficient (R^2) of the linearized form of Langmuir isotherm model was closest to unity, indicating that the adsorption process of all metal ions onto AcS, was correctly described by the Langmuir isotherm model. However, the maximum adsorption, qm values estimated by the Langmuir model corresponded to the experimental values obtained of qm_{exp}.

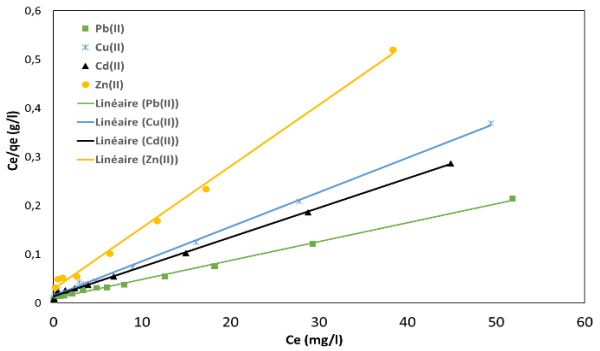

Fig. 10. The Langmuir isotherm of AcS.

Since adsorption was accompanied by evolution or absorption of heat depending upon the nature of adsorbent-metal interaction, the adsorption process was also dependent on temperature. Indeed, the thermodynamic parameters offered detailed information about the characteristic energy changes associated with the adsorption process.

Table 2. Langmiur and Freundlich adsorption isotherm parameters.

Metal ion	Langmuir			Freundlich		
	q ($mg.g^{-1}$)	K_L ($L.mg^{-1}$)	R^2	K_F ($mg.g^{-1}$)	n	R^2
Pb(II)	243.90	0.455	0.996	36.52	2.09	0.82
Cu(II)	140.84	0.476	0.997	20.46	1.91	0.90
Cd(II)	163.93	0.448	0.998	15.90	1.97	0.87
Zn(II)	79.36	0.433	0.996	14.01	1.55	0.93

To study the effect of temperature, the adsorption experiments were performed at 25, 35 and 45°C and the experiments have been realized under the same optimum conditions of concentrations, pH and contact time. The thermodynamic parameters including the free energy change ΔG^0, the enthalpy change ΔH^0 and the entropy change ΔS^0, were determined using the following equations:

$$\Delta G° = \Delta H° - T\Delta S° = -RTlnK_c \quad (10)$$

$$K_c = \frac{q_e}{C_e} \quad (11)$$

$$lnK_c = -\frac{\Delta H°}{R}\frac{1}{T} + \frac{\Delta S°}{R} \quad (12)$$

where Kc is the thermodynamic equilibrium constant, R (8.314 $J.mol^{-1}.K^{-1}$) is the general gas constant and T is the absolute temperature (K). The enthalpy change ΔH_0 and the entropy change ΔS_0 were obtained from the slope and intercept of the graph of ln (Kc) versus 1/T. From the results exposed in Table 4, the negative values of ΔG° indicated that the adsorption of metal ions onto AcS adsorbent was spontaneous and the adsorption decreased with an increase of temperature. The negative value of ΔH^o implied that the adsorption of metal ions onto AcS material was endothermic. The negative value of entropy change indicated a decrease in randomness at the adsorbate-solution interface during the adsorption process.

Table 3. Thermodynamic parameters of metal ion adsorption onto AcS.

Metal ions	R^2	$\Delta H°$ ($kJ.mol^{-1}$)	$\Delta S°$ ($J.K^{-1}.mol^{-1}$)	T (K)	$\Delta G°$ ($kJ.mol^{-1}$)
Pb(II)	0,995	-16.68	-44.39	298.15	-3.45
				308.15	-3.00
				318.15	-2.56
Cu(II)	0,995	-14.91	-40.07	298.15	-2.97
				308.15	-2.57
				318.15	-2.17
Cd(II)	0,996	-12.51	-31.67	298.15	-3.07
				308.15	-2.75
				318.15	-2.44
Zn(II)	0,994	-13.12	-37.68	298.15	-1.88
				308.15	-1.50
				318.15	-1.11

3.6.4 Competitive adsorption of metal ions and Regenerability of material

The adsorption selectivity of AcS toward Pb (II), Cu (II), Cd (II) and Zn (II) metal ions, was performed under the optimum condition, using a mixture of each metal ion Pb (II), Cd (II), Cu (II), Zn (II) and the results are presented in Figure 11.

The results showed a decrease in the quantity extracted compared to the value obtained in the absence of foreign metal ions and that made sense because in a single metal system there was no competition between metal ions for adsorption sites. However, the material showed selectivity to Pb (II) with an extraction capacity of 77. 48 $mg.g^{-1}$.

The stability of the adsorbent was studied by regeneration experiments. This procedure was necessary to evaluate the adsorption ability of material after the desorption process, and it enabled recovering valuable metals from wastewater streams. In the present work, Pb(II) was desorbed from modified cellulose acetate using 0.1 M HNO_3.

The results showed that the total decrease in terms of percentage adsorption after five cycles, were 9.5, 6.8, 8.4 and 5.88% for Pb(II), Cu(VI), Cd(II), and Zn(II), respectively. These results suggested the repeated use of material adsorbent before need to be changed.

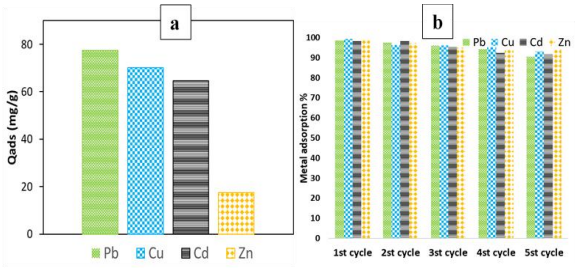

Fig. 11. Competitive adsorption of AcS(a) and Regenerability study(b).

4 Conclusion

The preparation of adsorbents as alternative to activated carbons in water treatment processes was one of the first interests in past ten years. An eco-friendly succinylated cellulose monoacetate adsorbent in its sodic form appeared highly efficient for the removal of Pb(II), Cu(II), Cd(II) and Ni(II) ions from aqueous solution. Effectiveness of the material had shown maximum adsorption capacity among the adsorbents based on polysaccharides in the literature reported until now as far as our knowledge is concerned.

The AcS showed an adsorption capacity of 241.64, 133.75, 156.23 and 73.91 $mg.g^{-1}$ for Pb(II), Cu(II), Cd(II), and Zn(II), respectively.

The adsorption process of metal ions onto AcS followed a pseudo-second-order kinetics and the equilibrium data have been well described by the Langmuir isotherm. The nature of the adsorption process was exothermic and spontaneous. These new materials can be used such as good alternative material for the metal ion removal from aqueous solutions and their stabilities were verified by regeneration study.

Reference

1. F. Fu and Q. Wang, J. Environ. Manage, **92**, 407-418 (2011)
2. A.P. Lim and A.Z. Aris, Reviews in Environmental Science and Bio/Technology, **13**, 163-181 (2014)
3. C. Achtel and T. Heinze, Macromolecular Chemistry and Physics, **217**, 2041-2048 (2016)
4. L. Lü, L. Chen, W. Shao, and F. Luo, Journal of Chemical & Engineering Data, **55**, 4147-4153 (2010)
5. I.H. Alsohaimi, S.M. Wabaidur, M. Kumar, M.A. Khan, Z.A. Alothman, and M.A. Abdalla, Chemical Engineering Journal, **270**, 9-21 (2015)
6. M. Hua, S. Zhang, B. Pan, W. Zhang, L. Lv, and Q. Zhang, Journal of Hazardous Materials, **211**, 317-331 (2012)
7. E. Repo, J.K. Warchoł, A. Bhatnagar, A. Mudhoo, and M. Sillanpää, water research, **47**, 4812-4832 (2013)
8. O.K. Júnior, L.V.A. Gurgel, R.P. de Freitas, and L.F. Gil, Carbohydrate Polymers, **77**, 643 (2009)
9. A. Razzaz, S. Ghorban, L. Hosayni, M. Irani, and M. Aliabadi, Journal of the Taiwan Institute of Chemical Engineers, **58**, 333-343 (2016)
10. M.M. Matlock, B.S. Howerton, and D.A. Atwood, Water research, **36**, 4757-4764 (2002)
11. C.A. Basha, M. Somasundaram, T. Kannadasan, and C.W. Lee, Chemical engineering journal, **171**, 563-571 (2011)
12. A.A. Nada and M.L. Hassan, Journal of Applied Polymer Science, **102**, 1399-1404 (2006)
13. L. Li, J. Dong, and T.M. Nenoff, Separation and Purification Technology, **53**, 42-48 (2007)
14. T.A. Kurniawan, G.Y. Chan, W.-H. Lo, and S. Babel, Chemical engineering journal, **118**, 83-98 (2006)
15. Z. Thong *et al.*, Environmental science & technology, **48**, 13880-13887 (2014)
16. X. Yu *et al.*, Journal of Environmental Sciences, **25**, 933-943 (2013)
17. T. Hajeeth, K. Vijayalakshmi, T. Gomathi, and P. Sudha, International journal of biological macromolecules, **62**, 59-65 (2013)
18. Y. Zhou, Q. Jin, X. Hu, Q. Zhang, and T. Ma, Journal of Materials Science, **47**, 5019-5029 (2012)
19. V. Renge, S. Khedkar, and V. Pandey Shraddha, Siences Review Chemical Communications, **2**, (2012)
20. A. Singha and A. Guleria, International journal of biological macromolecules, **67**, 409-417 (2014)
21. E.C. Silva Filho, L.C. Lima, F.C. Silva, K.S. Sousa, M.G. Fonseca, and S.A. Santana, Carbohydrate polymers, **92**, 1203-1210 (2013)
22. D.W. O'Connell, C. Birkinshaw, and T.F. O'Dwyer, Bioresource Technology, **99**, 6709-6724 (2008)
23. S. Hokkanen, A. Bhatnagar, and M. Sillanpää, Water research, **91**, 156-173 (2016)
24. L.V.A. Gurgel and L.F. Gil, Carbohydrate Polymers, 77, 142-149 (2009)
25. W. Li, R. Liu, H. Kang, Y. Sun, F. Dong, and Y. Huang, Polymer Chemistry, **4**, 2556-2563 (2013)
26. S. Kamel, E. Hassan, and M. El-Sakhawy, Journal of Applied Polymer Science, **100**, 329-334 (2006)
27. A. Elidrissi, S. El Barkany, H. Amhamdi, A. Maaroufi, and B. Hammouti, J Mater Environ Sci, **3**, 270-285 (2012)
28. X. Zhou et al., Cellulose, **23**, 811-821 (2016)
29. J. Li et al., Molecules, **14**, 3551-3566 (2009)
30. A.M. Das, A.A. Ali, and M.P. Hazarika, Carbohydrate polymers, **112**, 342-349 (2014)
31. J. Chen, J. Xu, K. Wang, X. Cao, and R. Sun, Carbohydrate polymers, **137**, 685-692 (2016)
32. R. M. Silverstein, F. X. Webster, D. J. Kiemle, and D. L. Bryce, John wiley & sons, (2014)
33. H. Kono, H. Hashimoto, and Y. Shimizu, Carbohydrate polymers, **118**, 91-100 (2015)
34. J. Luo and Y. Sun, Journal of applied polymer science, **100**, 3288-3296 (2006)
35. A.M. Senna, K.M. Novack, and V.R. Botaro, Carbohydrate Polymers, **114**, 260-268, (12/19/ 2014)
36. I. Jilal et al., Carbohydrate Polymers, (2017)
37. M. Iqbal, A. Saeed, and I. Kalim, Separation Science and Technology, **44**, 3770-3791 (2009)
38. I. Langmuir, Journal of the American chemical society, **38**, 2221-2295 (1916)
39. H. Freundlich, Zeitschrift für physikalische Chemie, **57**, 385-470 (1907)